A Journal of the Gesellschaft Deutscher Chemiker

Angewandte International Edition

GDCh

Chemie

www.angewandte.org

Accepted Article

Title: Tuning the selectivity of the catalytic CO2 hydrogenation reaction by strong metal-support interaction

Authors: Ding Ma

To be cited as: *Angew. Chem. Int. Ed.* 10.1002/anie.201705002
Angew. Chem. 10.1002/ange.201705002

Link to VoR: http://dx.doi.org/10.1002/anie.201705002
http://dx.doi.org/10.1002/ange.201705002

WILEY-VCH

Tuning the selectivity of the catalytic CO_2 hydrogenation reaction by strong metal-support interaction

Siwei Li[1†], Yao Xu[1†], Yifu Chen[1], Weizhen Li[1], Lili Lin[1], Mengzhu Li[1], Yuchen Deng[1], Xiaoping Wang[2], Binghui Ge,[3] Ce Yang[1], Siyu Yao[1], Jinglin Xie[1], Yongwang Li,[2] Xi Liu[2]* and Ding Ma[1]*

1. College of Chemistry and Molecular Engineering, Peking University, Beijing 100871, China, Email: dma@pku.edu.cn
2. Syncat@Beijing, Synfuels China Technology Co., Ltd, Beijing, 101407, China. Email: liuxi@synfuelschina.com.cn
3. Beijing National Laboratory for Condensed Matter Physics, Institute of Physics, Chinese Academy of Sciences, Beijing 100190, People's Republic of China

† These authors contribute equally to this work.

Abstract: A one-step ligand-free method based on absorption-precipitation process is developed to fabricate Ir/CeO_2 nano-catalysts. It is observed that Ir species have strong metal-support interaction (SMSI) with the cerium oxide substrate. Depends on the loading of Ir, the chemical state of iridium could be finely tuned. In CO_2 hydrogenation reaction, it was shown that the chemical state of iridium species, induced by SMSI, has a major impact on the reaction selectivity. We provide direct evidence that single site catalyst is not a prerequisite factor for the inhibition of methanation and sole production of CO in CO_2 hydrogenation reaction. Instead, the modulation of the chemical state of metal species by strong metal-support interaction is more important for observed selectivity regulation (metallic Ir particles for CH_4 while partially oxidized Ir species for CO production). It provides important understanding of heterogeneous catalysts at nano, sub-nano or atomic scales

To date, supported metal catalyst is one of the most investigated fields in heterogeneous catalysis due to its outstanding catalytic behavior in response to the rising challenges of environment and energy issues.[1] For example, catalytic hydrogenation of CO_2 towards designated products has drawn intensely interests,[2] as it could reduce emission of the greenhouse gas as well as produce chemical feedstock[3] or even fuels.[4] Previous studies demonstrate that catalytic performance of the supported noble metal catalysts is crucially influenced by particle sizes of the metals.[5] Regardless of enormous efforts devoted to prepare ultra-small nanoparticles or even 'single atom' catalysts with unique catalytic performance,[6] so as to study the size effect of nano-catalyst, the chemical characteristic of metal catalyst is sometimes overlooked. Indeed, the modification of the chemical state, for instance the oxidation state,[7] of the metal catalyst could influence the adsorption behavior of the reactants and the subsequent conversion of the reaction intermediates, and thus the reaction path. However, recently, there are only limited practices intended to tailor the catalytic selectivity of supported noble metals towards a given direction by tuning the chemical state of the noble metal nanoparticles.[8]

On the other hand, it has been evidenced that support can influence chemical state of noble metal nanoparticles in some ways other than simply acting as substrate for the dispersion of loaded metal.[9] In this work, a one-step ligand-free method based on absorption-precipitation is developed to synthesize highly dispersed Ir nanoparticles deposited on CeO_2 nano-platelets. The size of iridium species can be controlled below 2.5 nm even at very high Ir loading (20 wt%). It

was concluded that chemical state of iridium species can be tuned by varying the size of Ir nanoparticles supported on cerium oxide, which changes the selectivity to designated products in catalytic CO_2 hydrogenation reaction. By using various characterization methods, the insight of structure-property relationship on the Ir/CeO_2 catalyst is clearly revealed.

Controlling the size and especially the size uniformity of supported metal catalyst is a major challenge for study the catalytic structure-property relationship. To get mono-dispersed metal catalyst, shaping agents or surfactants that strongly bonded with metal surface are normally used, which sometimes mask the intrinsic catalytic behavior of the catalyst.[10] In current approach, the precursor of the Ir/Ce catalysts (Ir/Ce-OH) is prepared by a ligand-free absorption-precipitation synthetic method with $Ce(NO)_3$ and $IrCl_3$ as cerium and iridium sources and sodium hydroxide as precipitation agent, and no shaping agent or surfactant was used. The structure of obtained 20 Ir/Ce-OH (20 means Ir loading is 20wt%) was studied by XRD (Figure S1). Beside the peaks of cerium hydroxides, no diffraction associated with Ir species could be resolved, which suggests Ir species have strong interaction with the substrates, making it highly dispersed over cerium hydroxides even at relatively high Ir concentration. Indeed, TEM (Figure 1A) demonstrated that the sample was the aggregates of nanorods (by rolling of nano-sheets) with dimensions around 30 nm × 10 nm which was decorated with numerous 1.5 nm nanoparticles with narrow size distribution. The FFT pattern confirms the aggregates were cerium hydroxide nanocrystals, while the 1.5 nm nanoparticles were iridium species as conformed by HAADF-STEM image (Figure 1B). Surely, the facile synthesis method exhibits strong tolerance to the loading of Ir species, which will be discussed in below section.

It is interesting to know how those narrowly distributed iridium nanoparticles were formed. A series of characterization methods were used to follow the synthetic process. Ir 4f XPS spectrums (Figure 1C) were obtained to examine the oxidation state of iridium of 20Ir/Ce-OH sample taken out of the reaction mixture at different time intervals. However, during whole synthetic process (120 min) only the Ir^{3+} species could be resolved (at 62.5 and 65.7 eV), inferring that iridium species have not been reduced during the preparation process. At the same time, Ir L_3-edge EXAFS spectra (Figure 1D) were used for further understanding the bonding environment of Ir. Interestingly, with reaction proceeds, the intensity of Ir-Cl scattering gradually decreased while that of Ir-O scattering increased, indicating that $IrCl_3$ absorbed on cerium hydroxide nano-structure was precipitated by OH^- in the reaction mixture. It should be noticed that a considerable Ir-O coordinate shell is resolved at 1 minute, suggesting that the nucleation of iridium hydroxide is a fast process. As seen from TEM images, when the synthetic reaction was terminated at 1 minute, cerium hydroxide ultrathin nanosheets were observed (Figure S2), which were decorated with plenty of small iridium hydroxide nanoparticles. The ultrathin cerium hydroxide nanosheets provide abundant nucleation sites for iridium hydroxide and lead to homogeneous Ir/Ce-OH supported catalyst.

Before catalysis test, Ir/Ce-OH precursors (with 0.7 wt%, 5 wt%, 15 wt% and 20 wt% Ir loadings) were annealed in air and then reduced with dilute H_2 at 300 ^oC to get xIr/Ce catalyst (x means the weight loading of Ir). Ir/Ce catalysts after CO_2 hydrogenation reaction (300 ^oC, 10 h), termed as Ir/Ce-used, are examined by XRD and HADDF-STEM. XRD patterns of Ir/Ce-used catalysts were shown in Figure 2A. The diffraction peaks of CeO_2 dominate all of the catalysts. There is a broad peak at about 40 degree for 20 Ir/Ce-used catalyst and it became a small hump for 15 Ir/Ce-used catalyst, which is associated with metallic Ir species. However, this diffraction was

not found on 5 Ir/Ce-used catalyst, indicating that at this loading, even after reaction at 300 ^{o}C, Ir species were highly dispersed over the surface of cerium oxide. The size of Ir species in this catalyst and also those of higher Ir loadings is indeed very small. As detected by HADDF-STEM (Figure 2B-2D), the average size of Ir is 2.2 nm for 20 Ir/Ce-used, 1.6 nm for 15 Ir/Ce-used and 1.0 nm for 5 Ir/Ce-used, respectively (Figure S4). Significantly, there is no obvious aggregation or sintering of Ir nanoparticles after the reduction and CO_2 hydrogenation reaction. We believe that it is strong interaction between the support and active species [1a, 11] that stabilized the Ir species. The catalytic performance of these Ir/Ce catalysts for CO_2 hydrogenation reaction was evaluated at 300 ^{o}C (Table 1). Pure CeO_2 nanoparticles and commercial Ir/C catalysts are unable to catalyze CO_2 hydrogenation at 300 ^{o}C (Table 1, Entry 5 and 6), however, all the Ir/Ce catalysts are active for the CO_2 transformation reaction but show critically different selectivity to the products. To make a fair comparison of the selectivity, the conversion of CO_2 is controlled below 10%. 20 Ir/Ce catalyst exhibits very high selectivity towards methane (88%), indicating it is basically a methanation catalyst. However, a dramatic change in selectivity was observed on decreasing the Ir loading. For 15 Ir/Ce catalyst, the selectivity towards methane decreased to 56% while the rest of the product was CO. When the CO_2 conversion was changed under different reaction conditions, we found the selectivity of the different supported Ir catalysts was less influenced (see Figure S5 and Table S2 in the supporting material). This indicates that the hydrogenation ability of iridium species has been weakened which results in the formation of large amount of primary hydrogenation product, CO. When further decreasing the Ir loading to 5%, much to our surprise, the formation of methane was inhibited, with the product being pure CO (Table 1). For Ir/Ce catalyst with even lower iridium loading (0.7%), the CO selectivity keeps unchanged (Table 1, entry 4). This result indicates that the selectivity of CO_2 hydrogenation reaction can be tuned by simply changing the Ir loading.

As shown on XRD and STEM, the average sizes of small iridium nanoparticles on the various Ir/Ce-used catalysts ranges narrowly from 1 to 2.5 nm, in contrast to the crucial difference in their selectivity. As reported in reference,[6, 12] extremely small clusters catalysts with limited number of metal atoms or even single atoms possess distinctly different catalytic properties from the corresponding metal nanoparticle catalyst. It was attributed to the fact that those single site or small cluster catalysts does not match the site requirement for the formation of specific product. In the case of CO_2 hydrogenation reaction, it is proposed that CH_4 can only be formed on nanoparticle catalyst while single site catalyst is apt to produce CO.[6a-c] However, in our case, the selectivity to methane was completely switched off when the particle size of Ir drops from 2.5 nm to 1 nm. Clearly, we cannot attribute the block of deep hydrogenation path (to methane) to the insufficient catalytic sites on the surface, and instead, we believe that it is the chemical nature of the smaller particle instead of size of metal species that has the major impact on the catalytic selectivity.

In order to understand the reason behinds, EXAFS and XPS analysis were used to follow the change of used catalysts with different Ir loadings. In the Ir L_3 edge EXAFS (Figure 3B) spectrums, there are two major peaks at ~1.7 and 2.7 Å, which corresponds to Ir-O and Ir-Ir scatterings, respectively.[13] Obviously, for 20 Ir/Ce-used catalyst, the dominant feature is the Ir-Ir scattering (2.7 Å) (with coordination number, CN_{Ir-Ir}, of 9.7) assigned to metallic Ir species. With decreasing of Ir loading, CN_{Ir-Ir} gradually reduced from 9.7 for 20 Ir/Ce to 7.2 for 5 Ir/Ce (Figure 3A and Table S3). At the same time, the intensity of Ir-O scattering increase with the decrease of Ir

loading, as CN_{Ir-O} reaches 3.6 in case of 5 Ir/Ce-used catalyst, indicating that the Ir species on this catalyst was modified by oxygen atoms.[14] As the catalysts with different Ir loading underwent same treatment and reaction, the structural modification may come from the interplay between Ir species and CeO_2 substrate, which is well-known as strong metal-support interaction (SMSI).[15] As the surface state of the catalyst is more important for its catalytic behavior, the surface chemistry of the supported Ir catalysts were further evaluated by XPS (Figure 3C). For 20 Ir/Ce-used catalyst, the symmetric peak at ~60.5 eV in Ir 4f XPS spectrum is ascribed to metallic Ir.[16] Once the Ir loading decreased to 15%, the Ir 4f peak got broadened to some extent as well as the tip shifted to 60.7 eV. With further lowering the Ir loading to 5wt%, a 0.5 eV shift (61.0 eV) is observed as compared with 20 Ir/Ce-used, indicating that Ir species were partially positively charged.[17] Based on the EXAFS and XPS analysis, detailed information about the chemical properties of Ir nanoparticles with respect to the different Ir loading can be convincingly disclosed. As the particle size decreases, more oxygen atoms should be incorporated into the metal surface due to SMSI. The surface oxygen atoms could tune the chemical properties of Ir nanoparticles and therefore its catalytic performance. In order to obtain detailed evidences about incorporation of oxygen atoms in Ir nanoparticles without background disturbance from the oxide support, Electron Energy Loss spectroscopy (EELs) under STEM mode was used to directly collect both oxygen and iridium signals from Ir nanoparticles detached from CeO_2 support at atomic scales (Figure 3D-E and supporting materials Figure S6). A significant difference is observed between the oxygen K-edge spectra measured in single non-supported Ir nanoparticle from 20 Ir/Ce-used and 5 Ir/Ce-used catalysts. It proves that there is a considerable amount of oxygen atoms bonded to the Ir species of 5 Ir/Ce-used catalyst, while for 20 Ir/Ce-used catalyst, the Ir species are oxygen-free with metallic nature. This trend holds for catalyst with even lower Ir loading (Figure S7). The dominant feature in Ir L_3 edge EXAFS profile in this 0.7 Ir/Ce-used is the Ir-O scattering, demonstrating that coordination of oxygen atoms to the Ir species increased to a great extent (Figure S7C). XPS result further confirms nonmetallic nature of the Ir species (Figure S7D). Somehow, the size difference among the supported Ir catalysts with the different loadings might influence the catalytic performance as well since the smaller Ir nanoparticles have more under-coordinated atoms with higher chemical activity. Considering the evidenced strong interaction between the support and Ir nanoparticles (Figure 2 and Figure S4), a key role of CeO_2 can be then rationalized to be engineering the chemical properties of the support Ir catalysts due to the strong interaction between the support and Ir species.

From above results, obviously, the dispersion/chemical structure of the Ir species are pivotal for the selectivity of CO_2 hydrogenation reaction. Significantly, the existence of isolated metal sites is not a prerequisite factor for the inhibition of methanation and sole production of CO in CO_2 hydrogenation reaction. Instead, we believe that the reason behind the size effect is the modulation of the chemistry state of Ir species by the substrate, cerium oxide. It has been pointed out that the interaction between partially oxidized Ir nanoparticles and CO adsorbent is weaker than that between metallic Ir and CO.[18] In current case, while partially oxidized Ir/CeO_2 surface can catalyze the dissociative chemisorption and further reaction of CO_2, the desorption of resulted CO is apt to happen on this partially oxidized Ir species (than further dissociation/hydrogenation to get methane), giving a near 100% selectivity towards CO. It is worth noting that the isolated Ir species and the smaller Ir nanoparticles display the identical catalytic selectivity for CO (100%) in CO_2 hydrogenation reaction. Despite of a significant difference in dimensions (one is single metal, and

another one is 1 nm particle), the observation strongly suggests a similarity in chemical state of the two kinds of active sites, which work for CO_2 hydrogenation, but not CO hydrogenation. Regardless of very limited understanding about heterogeneous catalysts at sub-nano scales, enormous efforts have been devoted to fabrication of 'single-site' catalysts with great expectations on size-dependent properties. Our result suggests, beside this effect, the crucial influence of the strong interaction between the support and active species (SMSI) on the catalytic performance, which will diminish any difference arising from dimensional diversity at sub-nano scales.

Acknowledgement

This work was financially supported by the Natural Science Foundation of China (91645115, 21473003, 21222306, 21673273), National Key R&D Program of China (2017YFB0602200) and 973 Project (2013CB933100). XAFS experiments were performed at the Beijing Synchrotron Radiation Facility (BSRF) and Shanghai Synchrotron Radiation Facility (SSRF).

Reference:

[1] a) L. Lin, W. Zhou, R. Gao, S. Yao, X. Zhang, W. Xu, S. Zheng, Z. Jiang, Q. Yu, Y.-W. Li, C. Shi, X.-D. Wen, D. Ma, *Nature* **2017**, *544*, 80-83; b) Y. Zhai, D. Pierre, R. Si, W. Deng, P. Ferrin, A. U. Nilekar, G. Peng, J. A. Herron, D. C. Bell, H. Saltsburg, M. Mavrikakis, M. Flytzani-Stephanopoulos, *Science* **2010**, *329*, 1633-1636; c) M. Behrens, F. Studt, I. Kasatkin, S. Kühl, M. Hävecker, F. Abild-Pedersen, S. Zander, F. Girgsdies, P. Kurr, B.-L. Kniep, M. Tovar, R. W. Fischer, J. K. Nørskov, R. Schlögl, *Science* **2012**, *336*, 893-897.

[2] a) J. Klankermayer, S. Wesselbaum, K. Beydoun, W. Leitner, *Angew. Chem. Int. Ed.* **2016**, *55*, 7296-7343; b) E. V. Kondratenko, G. Mul, J. Baltrusaitis, G. O. Larrazabal, J. Perez-Ramirez, *Energy Environ. Sci.* **2013**, *6*, 3112-3135; c) W. Wang, S. Wang, X. Ma, J. Gong, *Chem. Soc. Rev.* **2011**, *40*, 3703-3727.

[3] a) M. D. Porosoff, X. Yang, J. A. Boscoboinik, J. G. Chen, *Angew. Chem. Int. Ed.* **2014**, *53*, 6705-6709; b) X. Yang, S. Kattel, S. D. Senanayake, J. A. Boscoboinik, X. Nie, J. Graciani, J. A. Rodriguez, P. Liu, D. J. Stacchiola, J. G. Chen, *J. Am. Chem. Soc.* **2015**, *137*, 10104-10107; c) Z. He, Q. Qian, J. Ma, Q. Meng, H. Zhou, J. Song, Z. Liu, B. Han, *Angew. Chem. Int. Ed.* **2016**, *55*, 737-741; d) J. Graciani, K. Mudiyanselage, F. Xu, A. E. Baber, J. Evans, S. D. Senanayake, D. J. Stacchiola, P. Liu, J. Hrbek, J. Fernandez Sanz, J. A. Rodriguez, *Science* **2014**, *345*, 546-550; e) S. Kattel, P. J. Ramirez, J. G. Chen, J. A. Rodriguez, P. Liu, *Science* **2017**, *355*, 1296-+; f) B. An, J. Zhang, K. Cheng, P. Ji, C. Wang, W. Lin, *J. Am. Chem. Soc.* **2017**, *139*, 3834-3840;

[4] a) G. Centi, S. Perathoner, *Catal. Today* **2009**, *148*, 191-205; b) J. Wei, Q. Ge, R. Yao, Z. Wen, C. Fang, L. Guo, H. Xu, J. Sun, *Nat. Commun.* **2017**, *8*, 15174; c) F. Wang, S. He, H. Chen, B. Wang, L. Zheng, M. Wei, D. G. Evans, X. Duan, *J. Am. Chem. Soc.* **2016**, *138*, 6298-6305; d) W. Ling, K. M. Stocker, G. C. Schatz, *J. Am. Chem. Soc.* **2017**, *139*, 4663-4666; e) X. Zhang, X. Li, D. Zhang, N. Q. Su, W. Yang, H. O. Everitt, J. Liu, *Nat. Commun.* **2017**, *8*, 1-9.

[5] a) A. Karelovic, P. Ruiz, *Appl. Catal. B* **2012**, *113*, 237-249; b) A. Karelovic, P. Ruiz, *J.Catal.* **2013**, *301*, 141-153.

[6] a) J. H. Kwak, L. Kovarik, J. Szanyi, *ACS Catal.* **2013**, *3*, 2449-2455; b) J. H. Kwak, L. Kovarik,

J. Szanyi, *ACS Catal.* **2013**, *3*, 2094-2100; c) J. C. Matsubu, V. N. Yang, P. Christopher, *J. Am. Chem. Soc.* **2015**, *137*, 3076-3084; d) H. C. Wu, Y. C. Chang, J. H. Wu, J. H. Lin, I. K. Lin, C. S. Chen, *Catal. Sci. Technol.* **2015**, *5*, 4154-4163.

[7] a) F. Che, S. Ha, J.-S. McEwen, *Angew. Chem. Int. Ed.* **2017**, *56*, 3557-3561; b) A. Marimuthu, J. Zhang, S. Linic, *Science* **2013**, *339*, 1590-1593.

[8] a) Y. Zhao, B. Zhao, J. Liu, G. Chen, R. Gao, S. Yao, M. Li, Q. Zhang, L. Gu, J. Xie, X. Wen, L.-Z. Wu, C.-H. Tung, D. Ma, T. Zhang, *Angew. Chem. Int. Ed.* **2016**, *55*, 4215-4219; b) J. C. Matsubu, S. Zhang, L. DeRita, N. S. Marinkovic, J. G. Chen, G. W. Graham, X. Pan, P. Christopher, *Nat Chem* **2017**, *9*, 120-127.

[9] a) S. Kattel, W. Yu, X. Yang, B. Yan, Y. Huang, W. Wan, P. Liu, J. G. Chen, *Angew. Chem. Int. Ed.* **2016**, *55*, 7968-7973; b) J. A. Rodriguez, D. C. Grinter, Z. Liu, R. M. Palomino, S. D. Senanayake, *Chem. Soc. Rev.* **2017**, *46*, 1824-1841.

[10] Z. Niu, Y. Li, *Chem. Mater.* **2014**, *26*, 72-83.

[11] a) X. Zhang, X. Zhu, L. Lin, S. Yao, M. Zhang, X. Liu, X. Wang, Y.-W. Li, C. Shi, D. Ma, *ACS Catal.* **2017**, *7*, 912-918; b) J. A. Farmer, C. T. Campbell, *Science* **2010**, *329*, 933-936; c) P. Chen, A. Khetan, F. Yang, V. Migunov, P. Weide, S. P. Stürmer, P. Guo, K. Kähler, W. Xia, J. Mayer, H. Pitsch, U. Simon, M. Muhler, *ACS Catal.* **2017**, *7*, 1197-1206;

[12] a) F. R. Lucci, J. Liu, M. D. Marcinkowski, M. Yang, L. F. Allard, M. Flytzani-Stephanopoulos, E. C. H. Sykes, *Nat. Commun.* **2015**, *6*; b) J. Liu, *ACS Catal.* **2017**, *7*, 34-59.

[13] H.-S. Oh, H. N. Nong, T. Reier, A. Bergmann, M. Gliech, J. Ferreira de Araújo, E. Willinger, R. Schlögl, D. Teschner, P. Strasser, *J. Am. Chem. Soc.* **2016**, *138*, 12552-12563.

[14] Z. Xu, F. S. Xiao, S. K. Purnell, O. Alexeev, S. Kawi, S. E. Deutsch, B. C. Gates, *Nature* **1994**, *372*, 346-348.

[15] S. J. Tauster, S. C. Fung, R. L. Garten, *J. Am. Chem. Soc.* **1978**, *100*, 170-175.

[16] H. N. Nong, L. Gan, E. Willinger, D. Teschner, P. Strasser, *Chem. Sci.* **2014**, *5*, 2955-2963.

[17] Y. Lykhach, S. M. Kozlov, T. Skala, A. Tovt, V. Stetsovych, N. Tsud, F. Dvorak, V. Johanek, A. Neitzel, J. Myslivecek, S. Fabris, V. Matolin, K. M. Neyman, J. Libuda, *Nat. Mater.* **2016**, *15*, 284-288.

[18] F. J. C. M. Toolenaar, A. G. T. M. Bastein, V. Ponec, *J. Catal.* **1983**, *82*, 35-44.

Table 1: The catalytic performance of Ir/Ce catalysts in the CO_2 hydrogenation reaction.[a] The comparison of the catalyst in this paper and references were listed in Table S1.

Entry	Catalyst	Ir wt %	CO_2 conv. %	CH_4 sele. %	CO sele. %	Activity. $mol_{co_2} mol_{Ir}^{-1} h^{-1}$

10.1002/anie.201705002

1	20 Ir/Ce	19.7	8.8	88	12	8.7
2	15 Ir/Ce	15.0	6.9	56	44	9.0
3	5 Ir/Ce	5.9	6.8	trace	>99	22.5
4	0.7 Ir/Ce	0.7	2.9	trace	>99	81.1
5	CeO_2	-	-	-	-	-
6	Ir/C	5.0	-	-	-	-

[a] Reaction conditions: 300 ^oC, catalyst (100 mg), $H_2/CO_2/Ar$= 76/19/5, 1.0 MPa.

10.1002/anie.201705002

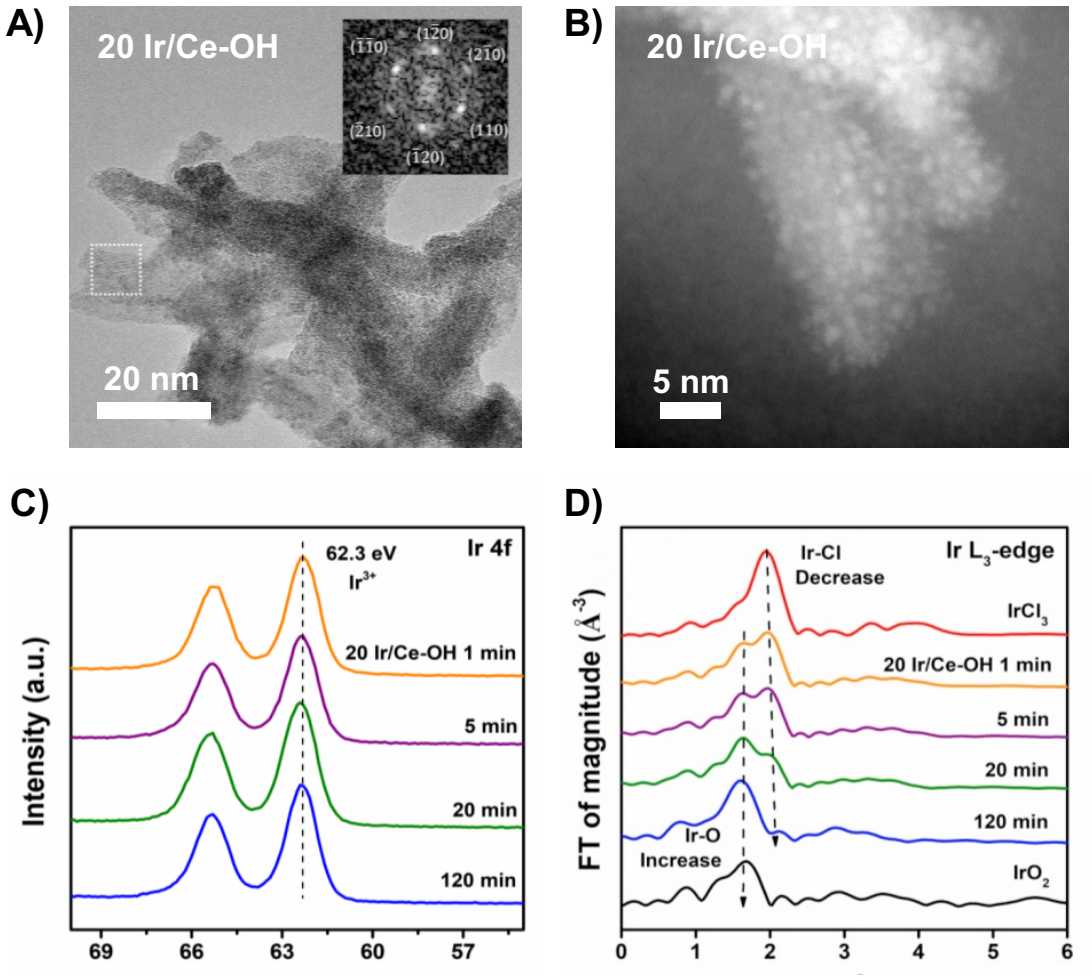

Figure 1. The ligand-free synthetic process of the 20 Ir/Ce-OH hybrid nanostructures. A) HR-TEM and SAED (inset), B) STEM of the 20 Ir/Ce-OH nanostructures. C) Ir 4f XPS spectrums and D) Ir L_3-edge EXAFS of the 20 Ir/Ce-OH nanohybrids taken out of synthetic mixture at different time interval.

10.1002/anie.201705002

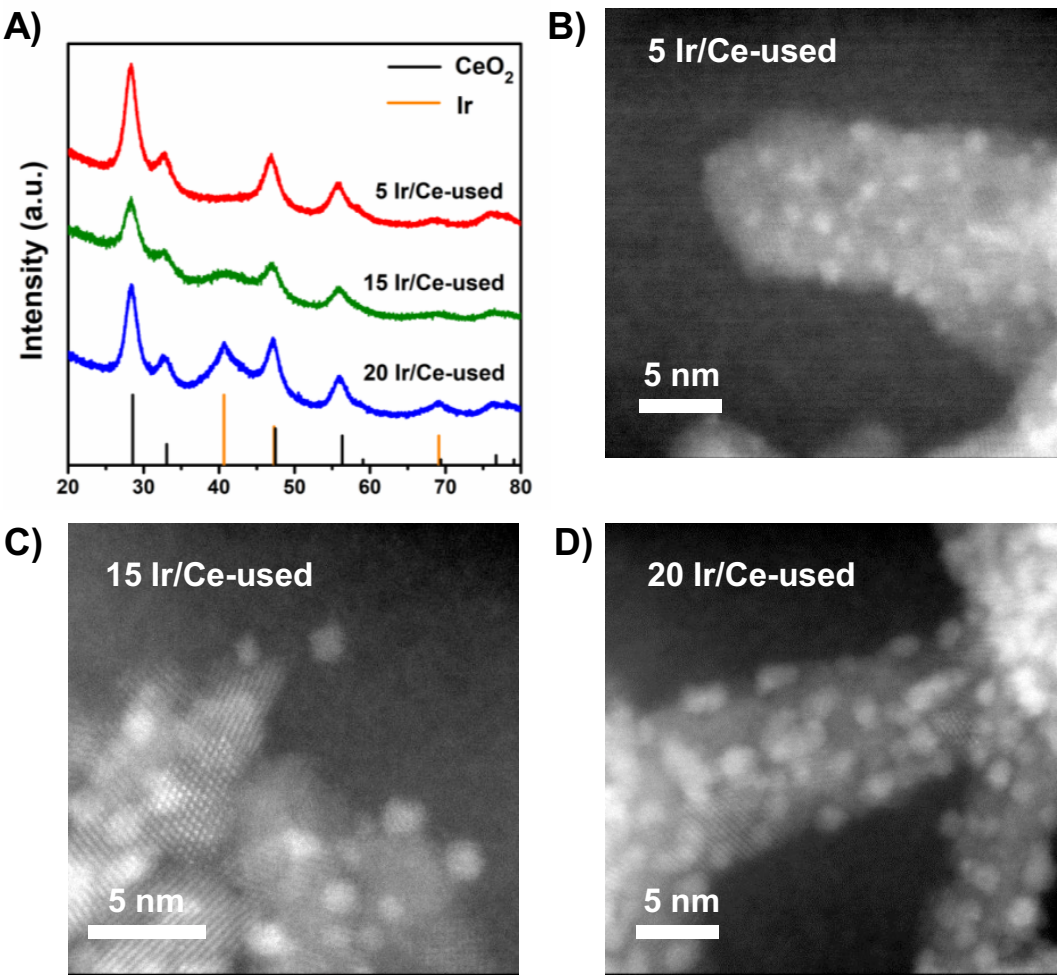

Figure 2. A) XRD patterns of the Ir/Ce-used catalysts with different Ir loading. STEM images of B) 5 Ir/Ce-used, C) 15 Ir/Ce-used and D) 20 Ir/Ce-used.

10.1002/anie.201705002

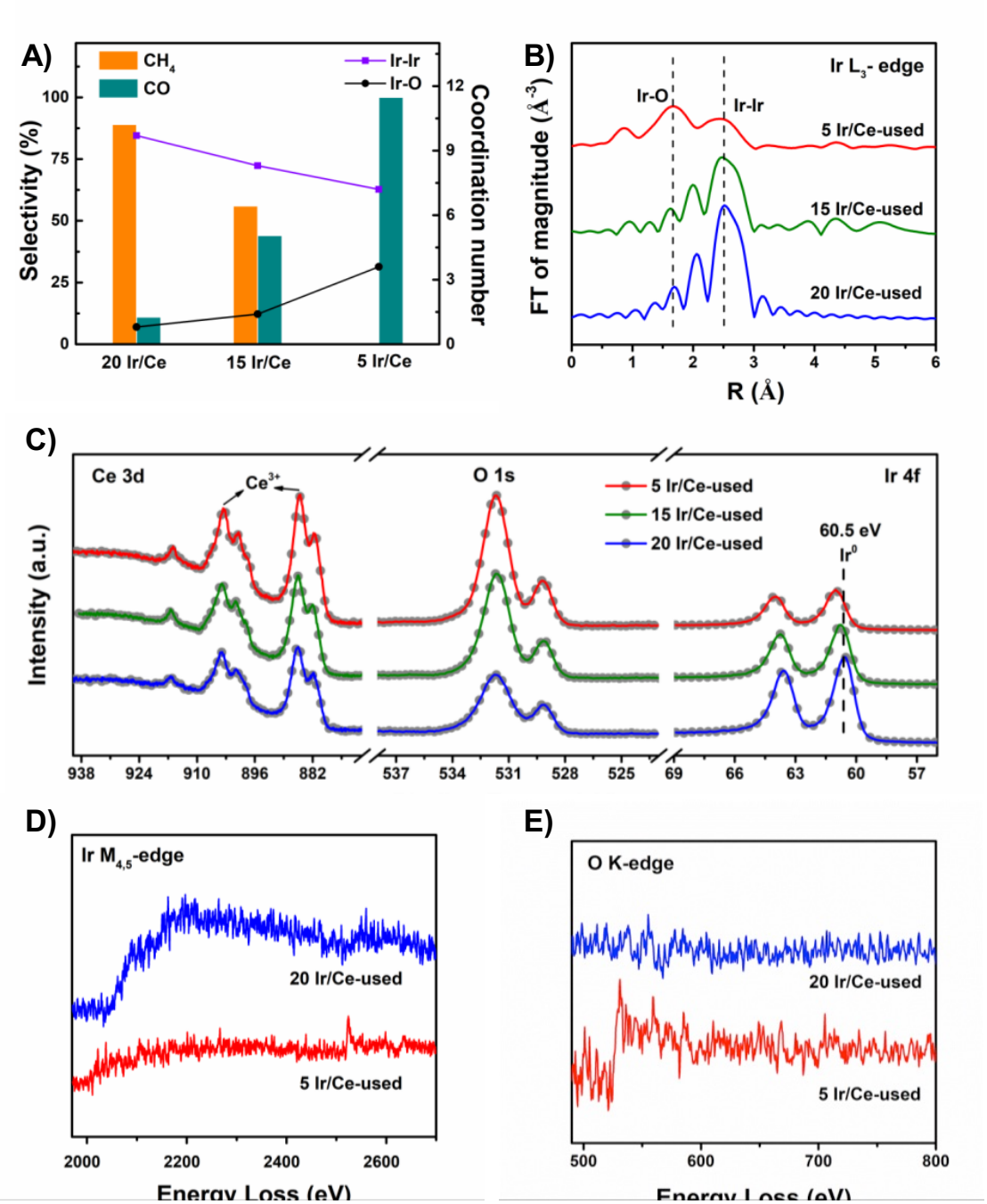

Figure 3. A) The coordination number (CN) of Ir-Ir and Ir-O shells (data, right axis) and their catalytic selectivity (bars, left axis) with Ir/Ce catalysts with different Ir loadings. B) Ir L_3-edge EXAFS of the Ir/Ce-used catalysts. C) XPS analysis of the Ir/Ce-used catalysts. D) and E) EELS of 5 Ir/Ce-used and 20 Ir/Ce-used.